بسم الله الرحمن الرحيم

Sudan University of Science & Technology

College of Petroleum Engineering & Technology

Petroleum Exploration Engineering Department

Graduation Project about:

Pore Pressure Prediction Using Seismic Method in Block 15 Red Sea

توقع الضغط المسامي باستخدام الطريقة السيزمية بمربع 15 – البحر الأحمر

Project submitted in partial fulfillment of requirement of the degree of B.sc (honor) in petroleum exploration engineering

Prepared by:

1. Mohammed Alnoor Aldegail Abdulrahman.
2. Sufian Hassan Mohammed Adam.
3. Reda Ismail Adam AbdelRahman.
4. Eltayeb Omer Alojaiba.

Supervisor:

Dr. Abbas Musa Yagoup.

October, 2015

Pore Pressure Prediction Using Seismic Method in block 15 Red Sea

توقع الضغط المسامي باستخدام الطريقة السيزمية بمربع 15 – البحر الأحمر

هذا المشروع مقدم إلى كلية هندسة وتكنولوجيا النفط – جامعة السودان للعلوم والتكنولوجيا

كإنجاز جزئي لأحد المتطلبات الأساسية لنيل درجة البكالوريوس مرتبة الشرف

في هندسة استكشاف النفط

إعداد الطلاب:

1. محمد النور الدقيل عبدالرحمن.
2. سفيان حسن محمد آدم.
3. رضا إسماعيل آدم عبدالرحمن.
4. الطيب عمر العجيبة.

مشرف المشروع:

- د. عباس موسى يعقوب   التوقيع ....

رئيس قسم هندسة الإستكشاف:

- أ. محمد عبدالله   التوقيع ....

عميد الكلية:

- د. تقوى أحمد موسى   التوقيع ....

التاريخ   /   / 2015

الآيـــــــــــة

قال تعالى:

(قُلْ اِعْمَلُوا فَسَيَرَى اللّهُ عَمَلَكُمْ وَرَسُولُهُ وَالمُؤمِنُون)

صدق الله العظيم

سورة التوبة: 105

Dedication

This project is dedicated to my father, who taught me that the best kind of knowledge is that which have a specific target. It is also dedicated to my mother, who taught me that even the largest task can be accomplished if it is done one step at a time. It's also **dedicated to the spirit of Dr. Mohammed Naeim** and to all our friends for their encouragement. Special thanks to our teachers and college.

Acknowledgments

We would like to sincerely thank our supervisor Dr. Abbas Musa for his patience, guidance and give us the opportunity to be our supervisor. We would also like to thank Sudapet Company for providing us with valuable advices their support for this project was greatly needed and deeply appreciated.

Abstract

The study has been made in the Red Sea area block15 to predict pore pressure of the formation using Eaton method which considered being one of the indirect methods of calculation and estimation of pressure. This method depends on seismic data and well data. The well selected is Talla-1 which located at the coordination of latitude °18 '50 with longitude of °38 '03. The well penetrates several formations which are Shagara, Wardan, Zeit and Dungunab formations. After calculation a plot has been created showing the relationship between pore pressure and depth which illustrate an increase of pressure with depth. Although this method provide us with information about the pore pressure but it's limited by several factors which is the quality of seismic data acquisition and processing also the complexity of subsurface structures.

التجريد

أجريت الدراسة في منطقة البحر الأحمر بمربع 15 لتوقع الضغط المسامي في الطبقات وذلك باستخدام طريقة إيتون والتي تعتبر إحدى الطرق غير المباشرة في حساب الضغوط وتقييمها والتي تعتمد على البيانات السيزمية وبيانات الآبار حيث تم اختيار بئر Talla-1 الواقع عند الإحداثيات خط العرض 50′ 18° مع خط الطول 03′ 38°. البئر يخترق عدة تكاوين وهي شجرة، وردان ، زيت و دنجناب.بعد الحسابات تم رسم علاقة بين الضغط المسامي مع العمق توضح زيادة الضغط مع العمق. على الرغم بإن هذه الطريقة تزودنا بمعلومات عن ضغط المسام ولكنها محكومة بعدة عوامل منها جودة البيانات السيزمية المكتسبة والمعالجة وأيضًا بالتراكيب الجيولوجية المعقدة تحت السطح.

Contents

List of Figures

List of Tables

Chapter One

Introduction

Chapter One

Introduction

Drilling is a key component of the petroleum industry. Pore pressure is a property of the formation that has direct impact on drilling and completion of wells.[3] Pore pressure which is the pressure exerted by fluids in the pores of a reservoir, normally hydrostatic pressure exerted by the column of water from the depth of the formation to sea level is a major issue faced by drillers in the exploration sector. Abnormal pore pressure can lead to very serious drilling incidents like well blowouts, fluid influx and could greatly increase non-productive drilling time if not predicted accurately while and before drilling. Seismic data has long been recognized as a mean of addressing shale pore pressure concerns without actually having a well at that particular location. The industry has limited control in the form of well logs and cores; these data provide a detailed look at a very small area. Seismic data gives a more general assessment of a larger area and, when calibrated with the existing well control provides a method for increasing the driller's confidence. Seismic data regardless of how it is processed does not directly measure pressure. Seismic interval velocities get influenced by changes rock properties and this is exhibited in terms of reflection amplitudes in seismic surveys. Consequently, velocity determination is the key to pore pressure prediction. However, when a correlation between seismic velocity and porosity can be established, then methods that can be used to estimate pore pressures are exist from the velocities. Pore pressure predictions calculated from wells and interval velocity data have been used almost exclusively to design well casings and drilling mud weight programs. However, it's also contains valuable information on how oil, gas and water is behaving in the subsurface and importantly how fluid pressures will effect top seals, fault seals and column heights in hydrocarbon prospects. Pressure information obtained while drilling may then be used to refine the acceptable region of parameter space, so that the best possible pore pressure prediction can be made ahead of the bit based on drilling information and seismic velocities. [8]

1.1 Basic Theories:

Prediction of pore pressure depends greatly on understanding of seismic and well characteristics for instance velocity, resistivity, and density which capture porosity changes during shale compaction under vertical loading. Pore pressure prediction's basic theory derived from Terzaghi's and Biot's effective stress law (Biot. 1941; Terzaghi 1996). This fundamental theory represents the formation pore pressure as a function of overburden stress and effective stress. Hottman and Johnson (1965) introduced the concept of using sonic velocities; also Pennebaker (1968) used interval velocities obtained from stacking velocities. Over the years, literature has been populated with works on the use of seismic data for predrill geopressure prediction of the various possible methods, the effective stress method has become the preferred standard widely used in the industry, with the most popular method being the Eaton method (Eaton, 1975) and the Bowers method (Bowers,1995). Another method using mean stress, developed by Harrold (2000) used comparable sand and shale structures at moderately low temperatures. [3]

1.2 Previous Studies:

Many studies have been made in the Red Sea by several researchers for example:

- Aswartiz & Arden in 1960, they have described the lithological history of Red Sea Area.

- Karilla & Scarb in 1962, they have drawn lithological maps, stratigraphic and biostratigraphic of Sudanese Red Sea Shorelines. According to their efforts and investigation as geologist in Agip Company that led to drill 6 wells.

- Sisteney in 1965 was the first one to realize and estimate the matching between Miocene and Paleocene, and tried to link systematically between stratigraphy of Red Sea and Gulf of Suez.

- Qurashi in 1971 with a team from Khartoum University enhanced the study using gravity survey maps from Atbara to Bortsudan.

- Chevron Company in (1975-1976) enhanced the study using gravity survey maps which led to results for correction maps of Bogair anomaly of Toker Delta area.

1.3 The Objective of Study:

The main objective of this study is to illustrate the possibility of using seismic data to predict pore pressure of formation by applying Eaton Method with integrating well logs data. The predicted pore pressure using seismic interval velocities and well logs of selected offset well which is Talla-1 from block15 in the Red Sea is to be compared with real pressure detected from drilling data.

1.4 Study Area Information:

Block15 covers an area of 24,377 km2, both onshore and offshore of Delta Tokar. With maximum water depth of 760m (2500 ft). [12]

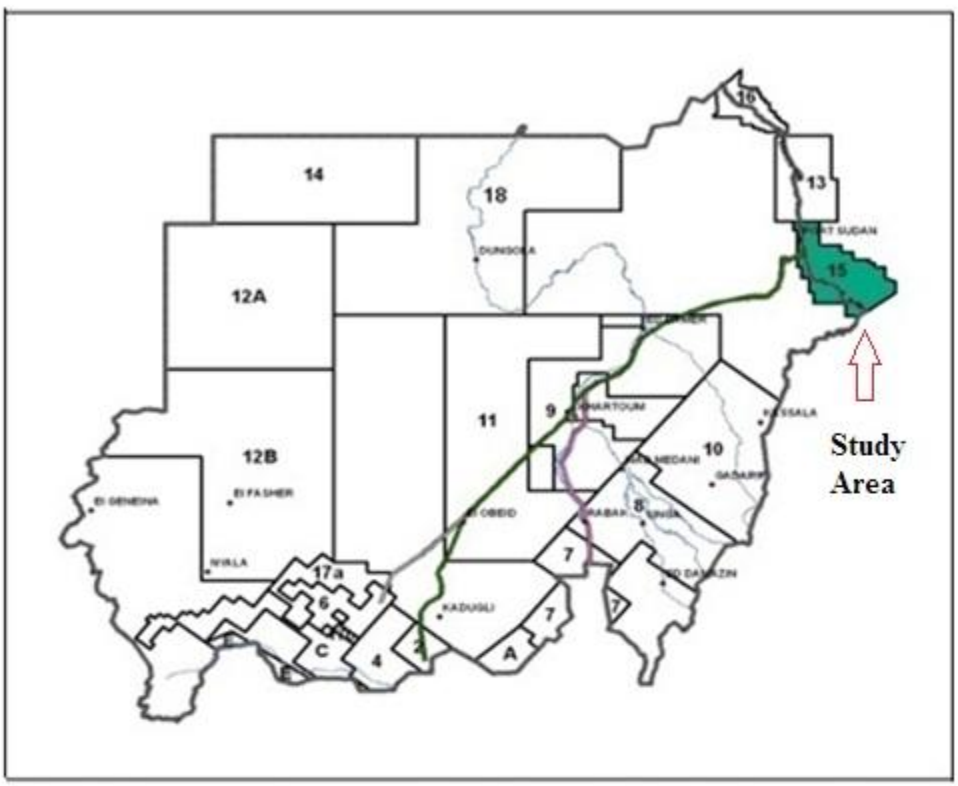

Fig (1.1): Map showing the location of Block 15 in northeastern of Sudan. [12]

1.5 Well under study: Talla-1 Well

The well type is Exploration Wildcat located nearby line IPS92-045. The coordinates are Latitude 18° 50’ 47” N and Longitude 38° 03’15” E. [12]

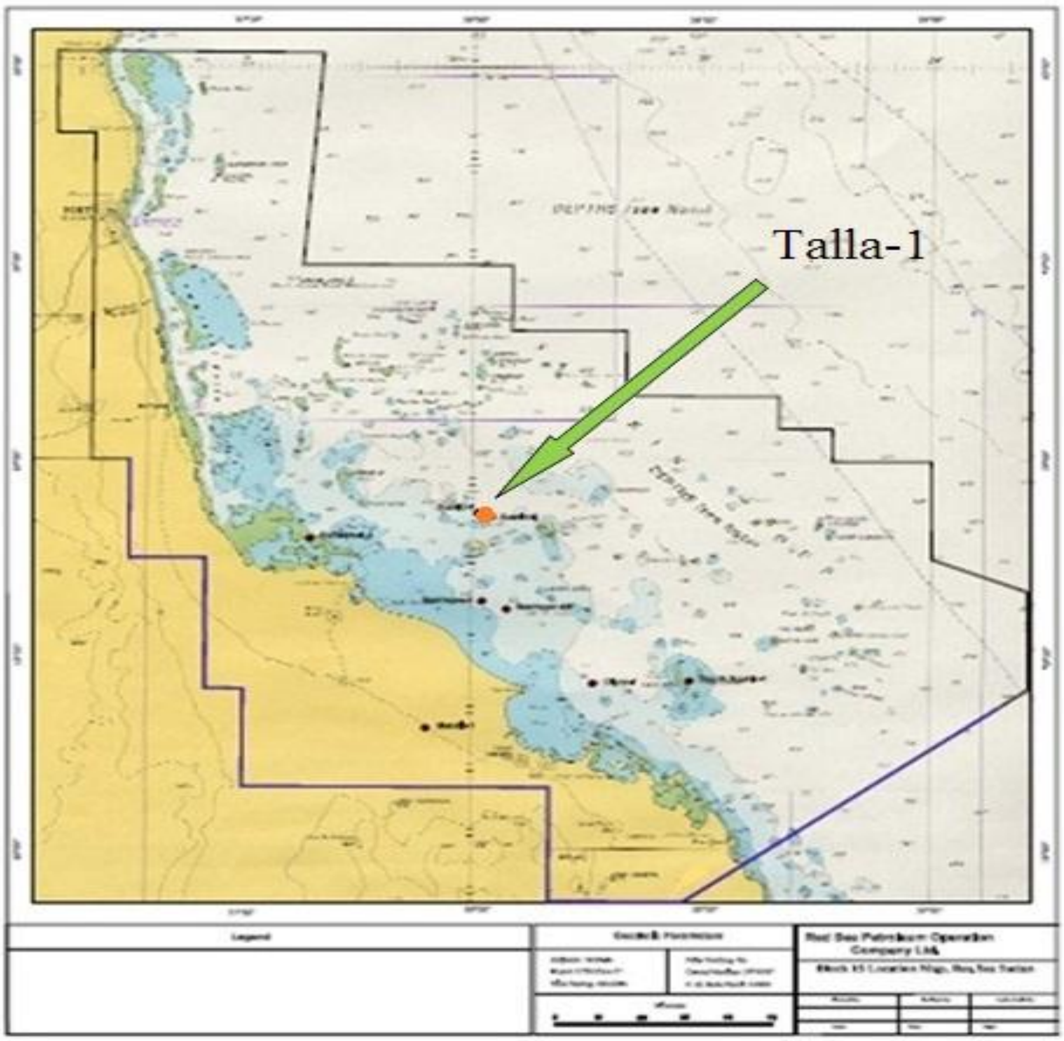

Fig (1.2): Geological Map showing the area of Block15.[12]

1.6 Data and Method of Analysis:

This project focuses on the prediction of pore pressure of the formations. In order to achieve that, data from the study area need to be obtained. These data according to the method are: a seismic data represented by the interval velocities of the layers and a well log data represented by the density log from which the overburden gradient will be calculated. By applying Eaton Method a plot represents the pore pressure related to the depth will be generated as a result using Excel software.

1.7 Rock Physics Depth Trends:

Velocity-depth trends are important in seismic exploration and borehole drilling for several reasons .Commonly. These have been used for detection of overpressure zones from seismic velocity (using travel time inversion).indicated by negative velocity (e.g., Herring. 1973:Japsen.dutta et al. 2002a, 2002b). These are important to detect since they can cause hazardous blowouts during drilling. Also, velocity-depth trends can be used for calculation of interval velocities and depth conversion and seismic time horizons (e.g. carter, 1989;Al-chalabi,1997) In areas where few wells are drilled , one often needs to assume a velocity trends based on an interpreted geologic depth column. The trends for sands and shales can also be used to study the expected seismic signatures of sand-shale interface as a function of depth, and to identify anomalous lithologies (e.g. limestones) digenetic zones(e.g., cementation). Similarly, over compacted zones related to uplift can be recognized, and erosion thickness (i.e., missing overburden) can be estimated (e.g., Bulat and Stoker, 1987; Japsen, 1993; Al-chalabi and Rosenkranz, 2002). Finally, expected brine-saturated velocity-depth trends can be applied to detect seismic velocity anomalies related to hydrocarbons (e.g., Avseth et al., 2003).

1.8 Rock Physics Properties as a Function of Compaction:

In order to understand the expected seismic response of a siliciclastic reservoir, at any given depth, it is key interest contrast in elastic properties between shales and sands as a function of depth. However, rock physics depth trends can be very complicated, depending on mineralogy, lithology, digenesis, pore pressure, effective stress and fluid properties. In areas with good well coverage, one can establish empirical rock physics depth trends for different lithologies from statistical regressions to well-log data (Vp,Vs, and density). [11]

In general, seismic velocities and densities of siliciclastic sedimentary rocks will increase with depth because of compaction and porosity reduction. However, the rock physics-depth trends can be rather complex because of the competing effects of porosity, pressure, mineralogy, texture and pore fluids. In fact, we may observe more than one cross-over in velocity-depth trends of sand and shales. Rock physics models can be very useful in better understanding these depth trends. However, the models have to be calibrated to local geology before they can be used for further prediction of hydrocarbons and lithology. Geologic constraints include expected lithofacies and association sand and shale mineralogy to determine effective elastic moduli and densities for the solid phase, fluid properties (oil density, GOR, gas gravity, brine salinity), as well as information about pressure and temperature gradients. [11]

1.9 Pressure Effects on Velocities:

There are at least four ways that pore pressure changes influence seismic signature: [11]

i. Reversible elastic effects on the rock frame.
ii. Permanent porosity loss from compaction and digenesis.
iii. Retardation of digenesis from overpressure.
iv. Pore fluid changes caused by pore pressure.

Chapter Two

Regional Geology of the Study Area

Chapter Two

Regional Geology of the Study Area

The Red Sea Basin area geographically includes the rifted sedimentary basins under several bodies of water, plus their tectonically related adjacent coastal regions. The first major Stratigraphic unit includes all igneous and metamorphic rocks of the “Basement Complex" which forms the Red Sea Hills and the foothills, and is generally considered to be of Precambrian age. See fig (2.1). In the "Basement Complex," Ruxton (1956) distinguished one metamorphic and two sedimentary and volcanic groups, separated by important unconformities, and affected by various kinds of intrusions.

2.1 The Basement Complex:

The term Basement Complex is normally applied to those complex of rocks of Pre-Nubian sandstone age. They are formed of metamorphic rocks, which exhibit variable degrees of metamorphism and include sediments from the Pre-Cambrian to Ordovician periods incorporated into a complex sequence of igneous intrusive and extrusive suits Robertson Research International, (RRI, 1984). The Basement Complex is considered the oldest rock unit exposed in northeastern of Sudan, which comprises the Red Sea Hills and the adjacent Nubian Desert. [9]

Oligocene continental rifting began with subsidence, extension and normal faulting associated with the episodic and segmented movement of the Arabian Peninsula away from Africa. Magmatic expansion resulted in igneous emplacements, and isostatic compensation caused the rift shoulders to undergo uplift and local erosion into the rapidly subsiding. [9]

2.2 Tectonic Setting:

A 5000 Km long orogenic belt was formed due to the collision named the East African Orogeny (EAO) (Stern, 1994). The belt consists of the Arabian Nubian Shield (ANS) in the north and the Mozambique belt to the south as shown in fig (2.2). [9]

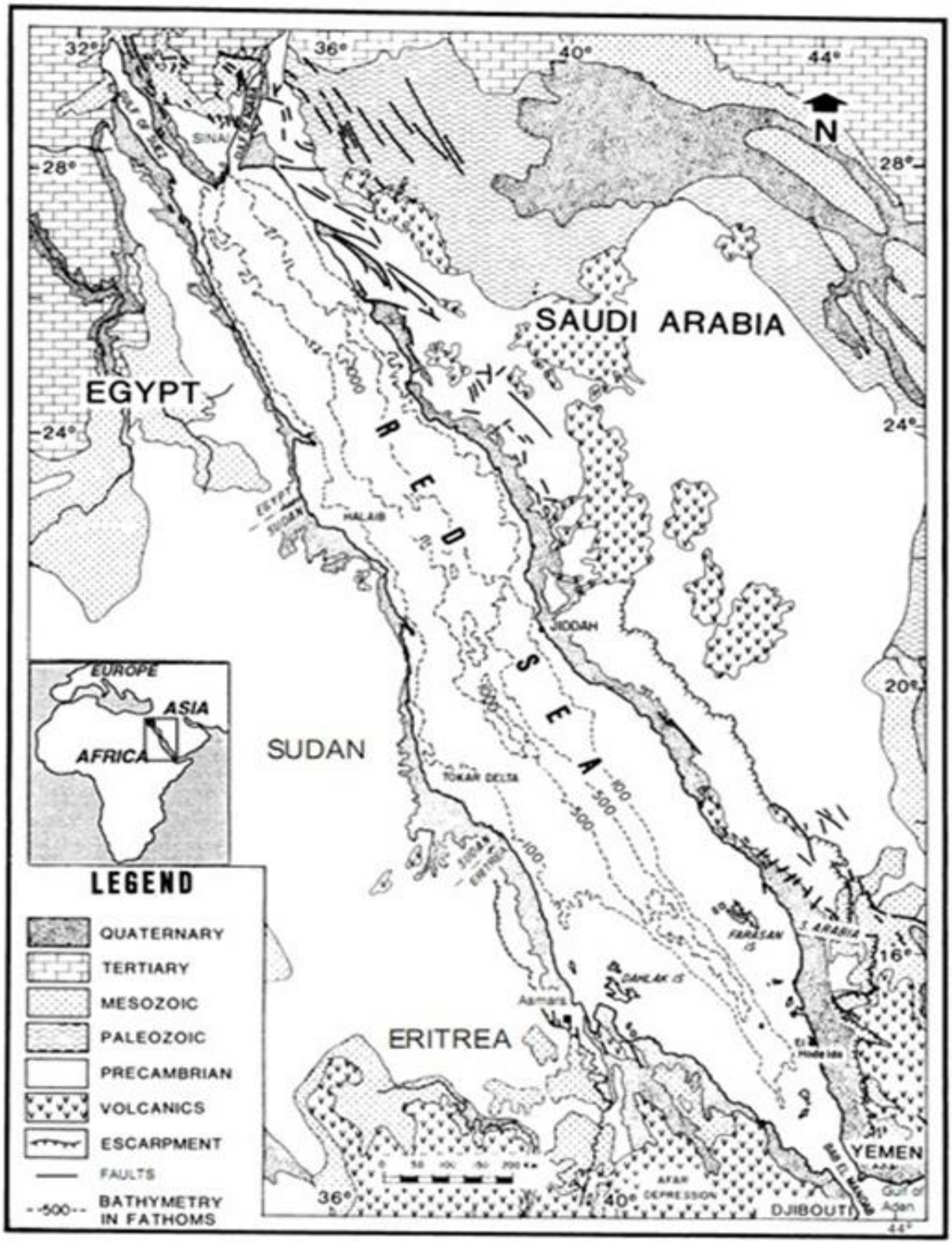

Fig (2.1): Index Map of the Red Sea region showing generlized geology and discussed location (after Mitchell and others, 1992).[12]

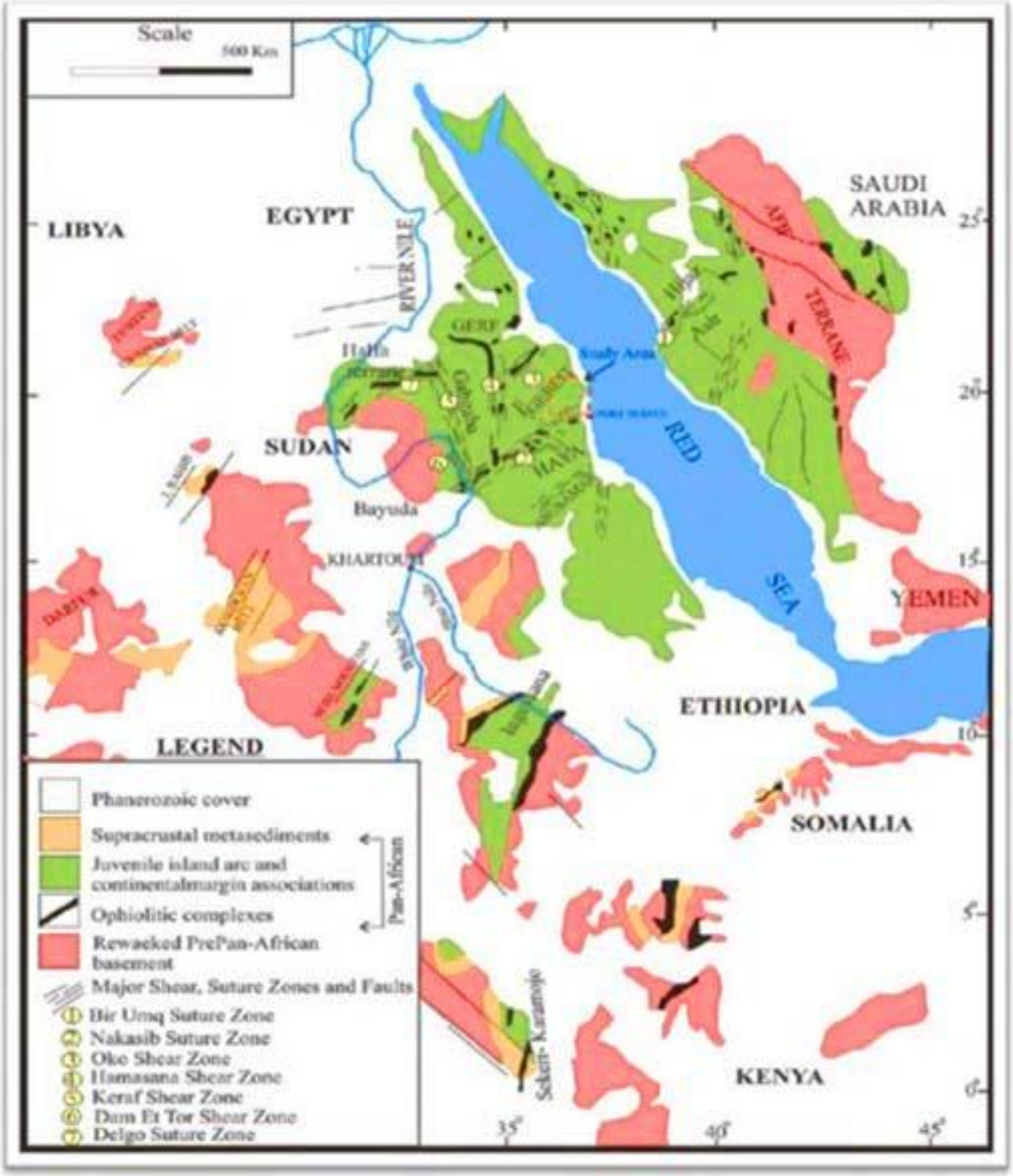

Fig (2.2): Geotectonic map showing the precambrian structures, the major suture and shear zones of the Arabian-Nubian Shield (ANS). (Modified after Abdelrahman, 1993 and Ali 2005)[12]

2.3 Regional Setting: Stratigraphy

i. Abu Shagara Group of Pliocene-Pleistocene:

Lower Unit Wardan Formation of coarse grained sandstone and gravel, with limestones, shales and dolomite. Upper Unit Shagara Formation of mainly carbonates with some shales and lesser sandstone.

ii. Zeit Formation of Upper Miocene:

Predominantly coarse to fine grained sandstone interbedded with shales, less anhydrite and minor thin carbonate beds.

iii. Dungunab Formation of Middle-Upper Miocene:

Mainly massive halite with anhydrite, lesser shale and very minor sandstone Varies in thickness from near shore to deeper water area.

iv. Belayim Formation of Middle Miocece:

The on/near shore is more clastic of sandstone & shale whereas in the open marine area, carbonate facies of mainly dolomite is prevalent.

v. Kareem Formation of Lower Miocene:

Shale interbedded with halite and minor sandstone in the upper unit. Evaporitic Markha unit of halite & anhydrite with some minor shales in the Lower unit.

vi. Rudeis Formation of Lower Miocene:

Interbedded shale and sandstone with minor limestone. Onshore area dominates by sandstone.

vii. Hamamit Formation of Lower Miocene – Paleocene:

Coarse quartzitic sandstone with lenses of conglomerates with volcanic fragments and basalt lava flows.

viii. Mukawar Formation of Upper Cretaceous:

Silty shale interbedded with fine-med grained sand stone, with subordinate marls and rare limestone.

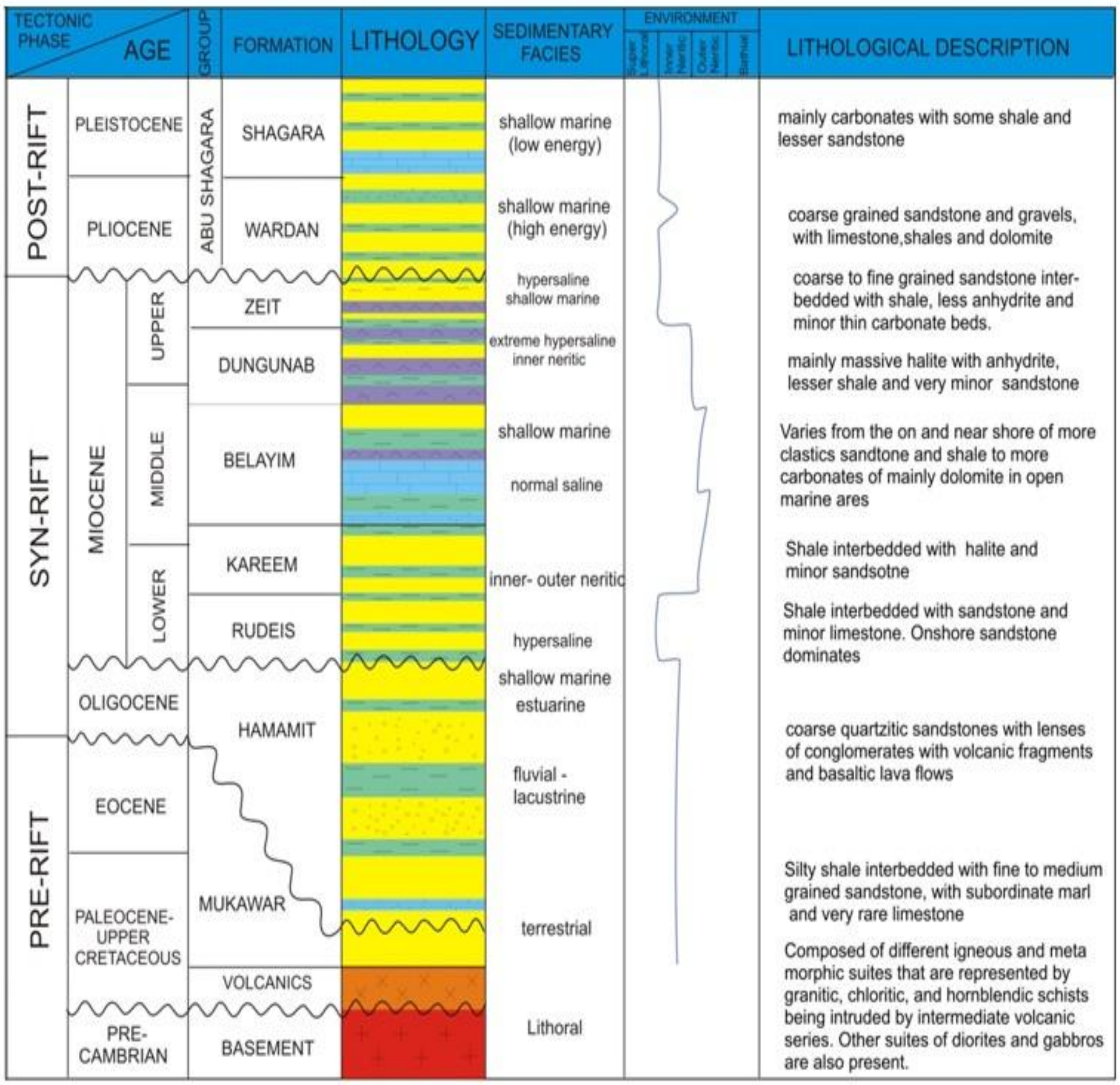

Fig (2.3): Red Sea Basin Generlized Straigraphic Column [12]

2.4 Exploration History:

Agip started exploration activities in the late 1950's and continue until 1963. Two wildcats and one appraisal wells were drilled during this period but no discovery was made. Exploration activities resumed when Chevron held the concession between (1975-1977), three wildcats were drilled, and two are discoveries (Bashayer-1A & Suakin-1) and one dry well. Between (1980-1982), two non-discovery wells were drilled by TOTAL and Union Texas. Suakin-2 was the last well drilled (by IPC in 1995). The last operator in the area was RSPOC, drilled two unsuccessful exploration wells in 2009 & 2010. Geological risk ranges from 1 in 8 to 1 in 10 with seal and trap as critical geological risk elements. [12]

2.5 Petroleum System: Reservoir & Seal

There are two parts in Block 15**:** [12]

Post Salt:

i. Zeit Formation: Consist mainly of fair to good quality reservoir in Suakin-1 & Bashayer-1A. The porosity is between 14-22% and the quality increases towards onshore.

ii. Dungunab Formation: Interbedded shale will provide the seal. The sealing efficiency increases toward offshore.

Pre Salt:

i. Belayem Formation: Upper member of Hamam Faraun has good reservoir quality in Durwara-2, Suakin-2 (sandstone) & Digna-1 (dolomite-porosity 17.5%).

ii. Rudeis Formation: Upper member has good reservoir quality in Durwara-2.

iii. Hamamit Formation: Two intervals contain very good quality reservoirs in Durwara-2 and Suakin-2.

iv. Mukawar Formation: Fair to good quality reservoir encountered in Maghersum-1.

v. Interbedded shale and salt will provide the seal.

2.6 Types of Traps:

There are four types of trap:- [9]

1. Roll-over structures as in Bashayer.
2. Slump structures created by down-dip sliding and crumpling of rocks in salt-lubricated slide planes as in Suakin.
3. Rotated fault blocks.
4. Stratigraphic.

2.7 Stratigraphy of the Well Formations:

Four of expected formations were penetrated in Talla-1. They were Shagara, Wardan, Zeit and Dungunab formations. However, the Belayim Formation remains inconclusive as no definite litho description data. Thus, the actual top Belayim would be subjected to outcome from further study. Some intervals in Dungunab Formation were difficult to be identified and interpreted due to presence of evaporate minerals in clastic sediments. Some of the interpreted lithology did not match with the original wells site descriptions. Preliminary wireline log interpretation suggested that there was a possibility of having salt cemented clastic lithology. [12]

i. Shagara Formation (51.8 – 986.8m TVDss):

Shagara Formation was picked at sea bed depth which is 52mTVDss. Shagara Formation consists of marine sand/sandstone section intercalated with Claystone. The Dolomite, Anhydrite and Limestone were present as streak layers.

ii. Wardan Formation (986.4m – 1410.8m TVDss):

Wardan Formation was picked at 986.4mTVDss based on the thickest Dolomite encountered. This is an indicative of different environment between Shagara and

Wardan. Wardan Formation consists of Sandstone, Siltstone, Claystone, Dolomite and series of Anhydrite.

iii. Zeit Formation (1410.8m – 2638.8m TVDss):

Preliminary Top of Zeit was picked at 1410.8m TVDss when the first thickest of evaporate (Anhydrite) was encountered in Talla-1 well. Generally Zeit formation consists of evaporites (Salt/Anhydrite), Sandstone, Siltstone and Shale.

iv. Dungunab Formation (2638.8m – 3336.8m TVDss):

Preliminary Top of Dungunab was picked when thick salt (~102m) was observed at 2638.8m TVDss. The Dungunab Formation is 648m thick consists of Salt and Anhydrite intercalated with Sandstone, Claystone and Siltstone.

Table (2.1): All the formation tops (Actual vs Prognosis) in Talla-1 are summarized as below table: [12]

FORMATION TOP	PROGNOSED DEPTH (m)		ACTUAL DEPTH (m)		DIF TVD
	MDRT	TVDss	MDRT	TVDss	(+Hi/-Lo)
Shagara	78.2	49.0	81.0	51.8	- 2.8
Wardan	1067.2	1038.0	1016	986.8	+ 51.2
Zeit	1869.2	1840.0	1440	1410.8	+ 429.2
Intra Zeit	2251.2	2212.0	2050	2020.8	- 191.2
Dungunab	2460.2	2431.0	2668	2637.9	- 206.9
Belayim	2809.2	2780.0	Not Firmed		
TD	3729.2	3700.0	3366	3336.8	+ 363.2

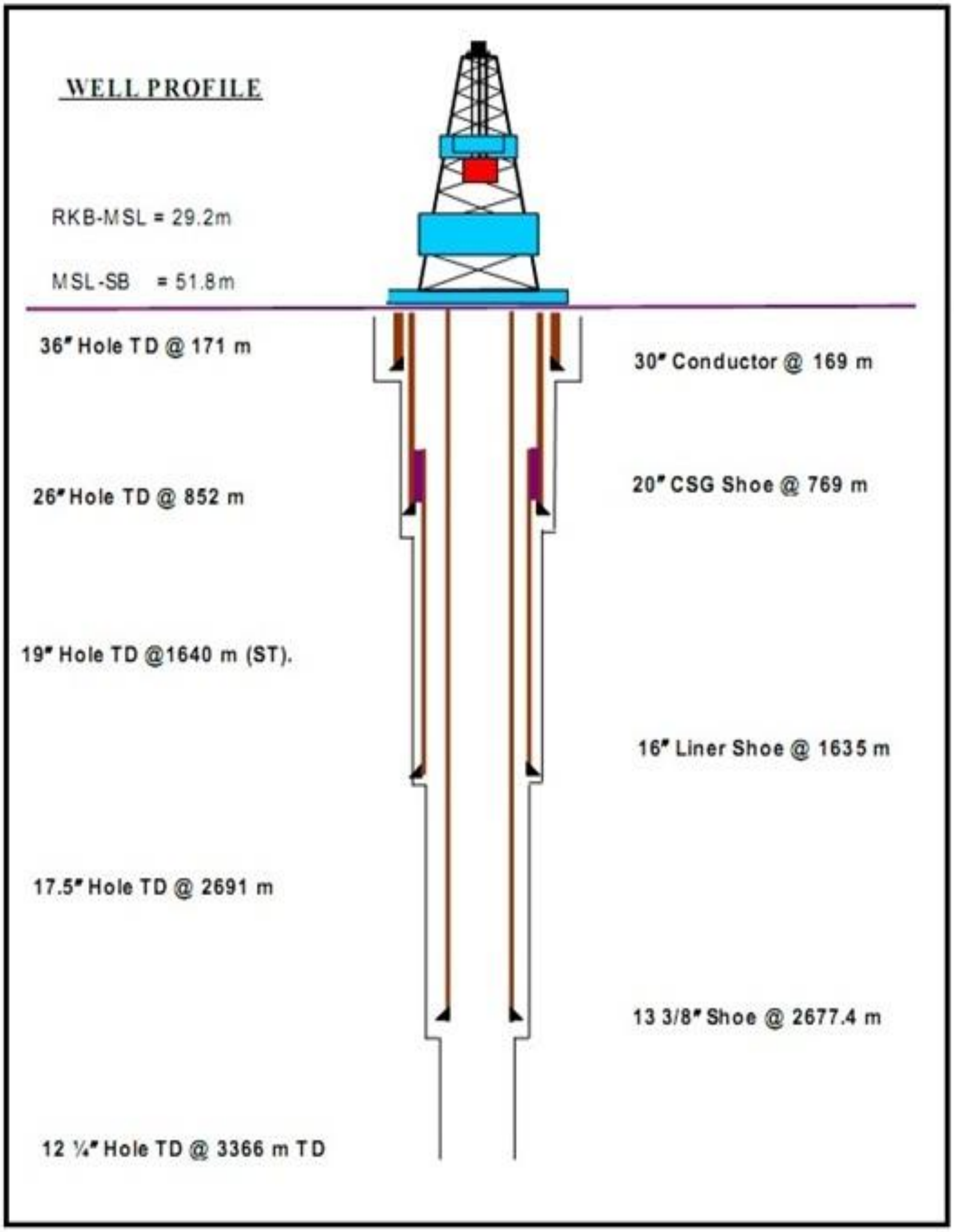

Fig (2.4): Talla-1 Well Schematic [12]

Chapter Three

Types of Pressures and Causes of Overpressure

Chapter Three

Types of Pressures and Causes of Overpressure

3.1 Types of Pressures:

The different formation pressures encountered in an area play a basic role both during exploration and exploitation of potential hydrocarbon resources reservoir. The different kinds of reservoir pressure which are usually encountered during the phase of drilling are broadly divided into three main components: [15]

i. Hydrostatic pressure.
ii. Overburden pressure.
iii. Formation pressure.

3.1.1 Hydrostatic Pressure (P_{hyd}):

It is defined as the pressure which is exerted by a column of water extending from a layer to a surface.

Hydrostatic pressure is caused by unit weight and vertical height of a fluid column.

The size and the shape of this fluid column have no effect on the magnitude of this pressure: [15]

$$P = \rho g h \quad \text{...} \quad (3.1)$$

where: P = hydrostatic pressure
ρ = average density
g = gravity value
h = height of the column

The hydrostatic pressure gradient is affected by the concentration of dissolved solids and the gases in the fluid column at different or varying temperature gradients. An increase in the dissolved solids slightly increases the normal pressure gradient, while increasing amount of gases in solution and higher temperature would decrease the normal hydrostatic pressure gradient. [15]

3.1.2 Overburden Pressure (P_o):

Overburden pressures are also sometimes called load, lithostatic or geostatic pressures. This pressure originates from the combined weight of the formation matrix (rock) and the fluids (water, oil, gas) in the pore space overlying the formation of interest.

$$P_o = \frac{weight\ (fluid + rock\ matrix)}{area}$$

but, weight of fluid = ρV

$$P_o = \frac{\rho_{fl}\phi(Ah) + \rho_{ma}(1-\phi)(Ah)}{A}$$

$$P_o = h\left[\phi\rho_{fl} + (1-\phi)\,\rho_{ma}\right] \quad \text{………………….. (3.2)}$$

Where:

Po = Overburden Gradient.

h = Thickness.

$\emptyset$ = Porosity.

ρ_{fl} = Fluid Density.

ρ_{ma} = Matrix Density.

Sediment porosity decreases under the effect of compaction which proportional to the increase in overburden pressure. In the case of clays, this reduction is essentially dependent on the weight of the sediments. If clay porosity and depth are represented on arithmetical scales, the relationship between these two parameters is an exponential function. In sandstones and carbonates, this relationship is a function of many parameters other than compaction, such as diagnostic effects, sorting, and original composition. a decrease in porosity is necessarily accompanied by an increase in bulk density. [15]

The total of overburden pressure is supported by:

i. Pore pressure.
ii. Rock gain pressure.

i. Pore Pressure:

The pore pressure of a formation refers to that portion of the overburden pressure which is not supported by the rock matrix, but rather by the fluids or gases which exist in the pore spaces of the formation. [15]

Normal pore pressure is equal to the hydrostatic pressure of a water column from that depth to the surface. If for some reason communication between fluids contained at depth and surface fluids is interrupted, fluids will be unable to flow and normally equal the pressures within the system. Thus fluids become entrapped within the formation and, in the case of over pressured formation, the grain to grain pressure decreases as the fluids with the interstices effectively "floats" the overburden. If the pore pressure is less than normally hydrostatic pressure the formation said to be subnormally pressured. If the pore pressure at that depth exceeds the expected hydrostatic pressure for that depth the zone is termed abnormally pressured. [15]

ii. Rock Grain Pressure:

Rock grain pressure refers to a theoretical fraction of the overburden pressure which is supported by the rock matrix of the formation.

Since a rock mass is not homogeneous, pressures will not be exerted equally in all directions as is the case with fluids pressures. [15]

3.1.3 Formation Pressures (P_f):

P_f is the pressure acting upon the fluids (water, oil, gas) in the pore space of the formation (pore pressure = formation fluids pressure). Expressed in psi, atmosphere or kg\cm^2.

Normal formation pressure in any geologic setting will equal the hydrostatic top of water from the surface to the subsurface formation.

Normal hydrostatic reservoir pressures normally correspond to original reservoir pressures. Any deviation from the normal trend is called abnormal. [15]

3.2 Pressure Relations:

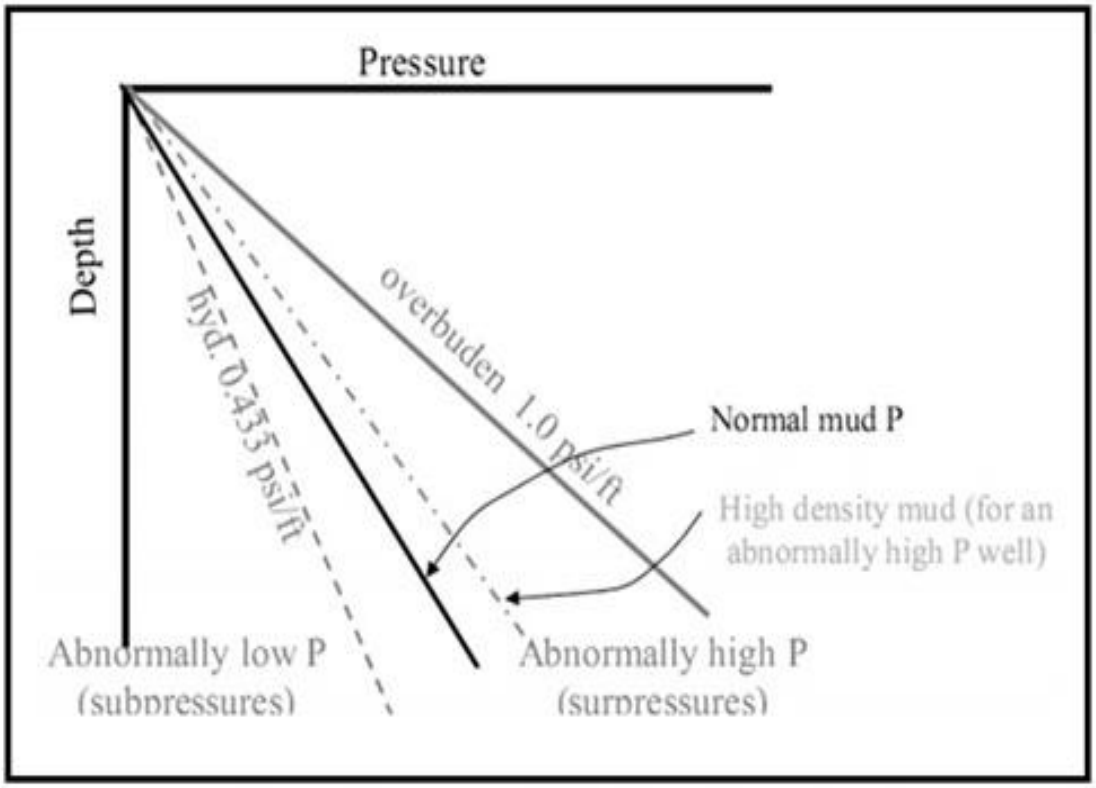

Fig (3.1): Pressure relation plotted with depth [15]

Pressures could be differentiated from normal pressure as shown in Fig (3.1) into: [15]

i. If $P_f > P_{hyd}$: abnormal pressure (surpressures/overpressures).
ii. If $P_f < P_{hyd}$: subnormal pressure (sub pressures).

surpressures occurring more frequently than subpressure.

3.3 Causes of Overpressure:

Overpressures in sedimentary basins have been attributed to different mechanisms but the main ones are related to increase in stress and in-situ fluid generating mechanisms. The ability of each of these processes to generate overpressures depends on the rock and fluid properties of the sedimentary rocks and their rate of change under the normal range of basin conditions. [7]

3.3.1 Primary Pressure Mechanisms:

Increase in stress during deposition of sediments, with the increase in vertical stress, the pore fluids escape as the pore spaces try to compact. If a layer of low permeability prevents the escape of pore fluids at rates sufficient to keep up with the rate of increase in vertical stress, the pore fluid begins to carry a large part of the load and pore-fluid pressure will increase. This process is referred to as undercompaction or compaction disequilibrium.

3.3.2 Secondary Pressure Mechanisms:

These mechanisms are also called unloading mechanisms because they tend to cause the in-situ pore pressure to increase at a fixed overburden, which results in a decrease in the effective stress on the matrix, hence the term unloading and it is include: [7]

i. Fluid Expansion Unloading Mechanisms:

Over pressure in the pore spaces of a formation can result by fluid expansion mechanisms as the rock matrix constrains the increased volume of the pore fluid. These include processes like heating, clay dehydration (Dutta, 1987), hydrocarbon maturation.

ii. Lateral Transfer:

When sediments under any given compaction condition has fluid injected into it from a more highly-pressured zone a fluid expansion occurs.

iii. Structural Uplift:

A very dangerous form of unloading occurs when sediments are uplifted by tectonic activity. Uplift of sediments alone will not cause unloading if the overburden load is not changed, but when the overburden is reduced during uplift either by syn-depositional tectonic processes or by erosion, the accompanying reduction in overburden results in the original in-situ pore pressure being contained by a much lower overburden, which results in a reduction of the effective stress, and unloading. [7]

3.4 Hydrocarbon Gradient:

The presence of hydrocarbons in the pore fluid column will cause variations in the pore fluid gradients, and therefore in the magnitude of the pore pressure. [15]

3.5 Drilling problems associated with abnormal pressures:

When drilling through formation, sufficient hydrostatic mud density must be maintained to prevent: [15]

i. The borehole collapsing.
ii. The influx of formation fluids.

If the over balance is too great, this may lead to:

i. Reduced penetration rates (due to cuttings hold down effect).
ii. Lost circulation (flow of mud into formation).
iii. Breakdown of formation (exceeding the fracture gradient).
iv. Excessive differential pressure causing stuck pipe.

Chapter Four

Pore Pressure Prediction Methods

Chapter Four

Pore Pressure Prediction Methods

4.1. Indirect Pressure Measurements (Prediction Methods):

4.1.1 Ben Eaton Method:

Eaton Interval Velocity of seismic data;

The following observational mathematical statement was displayed by Eaton (1975) from Interval Velocity of seismic data for pore pressure prediction;

$$PP = OBG - [(OBG - Phyd)\ (V/Vn)\ ^\wedge\ n] \quad \text{……………………} \quad (4.1)$$

Where:

PP = Pore pressure.

OBG = Overburden gradient.

Phyd = Hydrostatic pressure (typically 0.45 psi/ft or 1.03 Mpa/km, reliant on the salinity of water).

Vn = Interval velocity at the normal trend.

V= Interval velocity measured.

4.1.2 Eaton Resistivity:

Under compaction is the primary driver of overpressure in young sedimentary basins e.g North Sea, Gulf of Mexico. This approach is applied essentially for young sedimentary basins, where the normal shale resistivity is calculated correctly. Assuming that the normal shale resistivity is constant, is one methodology, accurate determination of the normal compaction trend line is an alternate method of determining pore pressure. [16]

Eaton (1972, 1975) gave the accompanying mathematical statement for pore pressure gradient prediction in shales utilizing resistivity log;

$$PP = OBG – [(OBG – Phyd) (R/Rn) ^ n] \quad …………………..……. (4.2)$$

Where:

Rn = Shale resistivity at ordinary (hydrostatic) pressure.

R = Shale resistivity acquired from well log.

n = an exponent which differs from 0.6 to 1.5, and normally n = 1.2

4.1.3 Bowers Method:

It represents a relationship between effective stress and velocity that could be utilized to associate seismic/sonic travel time to formation pore pressure. An input parameter maximum velocity depth, dmax, determines if unloading has happened or not utilizing this approach. Unloading has happened, If dmax is short of what the depth (Z) is the pore pressure can be gotten utilizing the equation: [16]

$$PP = OBG – 1/c \ln [(Vm– Vml) / (Vm – Vp)] \quad ……………… (4.3)$$

Where:

Vm= sonic interim velocity in the shale matrix. (Vm = 14,000 – 16,000 (ft/s))

Vp = the compressional velocity at a given depth.

c = experimental parameter that characterizes the rate of increase in velocity with effective stress (usually 0.00025).

dmax = the depth at which the unloading has happened.

OBG = overburden stress.

4.1.4 The D Exponent Methodology:

The method was proposed by Jordan and Shirley (1966) based on the bingham (1969) equation, which was developed to consider the differential pressure effect in normalizing penetration rate. [16]

The D exponent equation calculated from:

$$D= [((\log(R/60*N))/(\log(12W/10^{\wedge}*B))]*(\rho_{normal}/\rho_{actual}) \quad \ldots\ldots\ldots\ldots (4.4)$$

Where:

D = D exponent.

R = Penetration rate (ft/h).

N = RPM (Revolutions per minute).

B = Bit diameter (in).

W = Weight on the bit.

ρ_{normal} = Normal Hydrostatic gradient (ppg).

ρ_{actual} = Current mud weight (ppg).

$$PP = OBG - [OBG - Pn]*[D/Dn] \wedge b \quad \ldots\ldots\ldots\ldots (4.5)$$

Where:

P = Pore Pressure.

Pn = Normal pressure.

OBG = Overburden Pressure.

Dn = Normal trend of the D exponent.

4.1.5 Equivalent Depth Method:

The Equivalent depth approach is an example of the analysis utilizing trend line. A depth section is first assumed in this method where the pore pressure is hydrostatic, and the sediments are generally compacted due to the deliberate rise in effective stress with depth. Normal Compaction trends (NCTs) might be shown as straight lines fitted to the data over the ordinarily compacted interim after the log of a measured quality are plotted as a function of depth. Pore pressure at any depth where the measured value is not on the NCT (Normal compaction trend) could be calculated from the equation below as the value of the measured physical property is a distinct function of effective stress. [16]

$$Pb = Pd + (Sz - Sa) \quad \ldots\ldots\ldots\ldots\ldots\ldots\ldots\ldots\ldots\ldots\ldots \quad (4.6)$$

Where:

PP_b = Pore pressure at b.

PP_d = Pore pressure at d.

S_b = Stress at b.

S_d = Stress at d.

b = depth of interest.

d = depth along the normal compaction trend at which the measured parameter is the same as it is at the depth of interest Effective stress is a linear function of profundity, this is the main significant presumption needed when the equivalent depth system is utilized.

4.1.6 Ratio Method:

Here, pore pressure is computed based on the supposition that for resistivity, sonic delta-t, and density singly, the pore pressure is as a result of the normal pressure increased (multiplied) or separated by the degree (ratio) of the measured value to the normal value for the same depth. [16]

$$PP = P_{hyd}\,\Delta T_{log} / \Delta Tn \quad (4.7)$$

$$PP = P_{hyd}\,\rho n / \rho_{log} \quad (4.8)$$

$$PP = P_{hyd}\,Rn / R_{log} \quad (4.9)$$

The subscripts n and log indicate the normal and measured values of resistivity, density, or sonic delta-t, P_{hyd} is the normal hydrostatic pore pressure and PP is the real pore pressure.

Calibration of this approach needs knowledge of the right typical value of every parameter. It is vital to perceive that in distinction of trend line systems, the ratio approach doesn't utilize effective stress or overburden explicitly thus is not an effective stress methodology. This can result in unphysical conditions, where the overburden is lower than the computed pore pressure.

4.1.7 Tau Method:

Shell proposed a pore pressure prediction technique that depends on velocity as it introduced a "Tau" variable in the mathematical statement of effective stress (Lopez et al., 2004; Gutierrez et al., 2006);

$$Se = As*T*Bs \quad (4.10)$$

Where:

As and Bs = the fitting constants.

T = The Tau variable.

T = (C – Dt) / (Dt –D).

Dt = the compressional travel time either from seismic velocity or sonic log.

C = the constant associated with the travel time (mudline) (typically C = 200 ms/ft).

D = constant associated with the travel time (matrix) (normally D = 50ms/ft).

The pore pressure can be computed from the equation below:

$$P = OBG - As\,[(C - Dt) / (Dt - D)]\,Bs \quad (4.11)$$

4.1.8 Field Method:

This is utilized for the most part when formation pressure is due to under compaction. The formation liquid underneath the boundary must support the rock matrix, formation liquids and overburden, in the event that it is assumed that compaction does not take place beneath the boundary depth. The pressure is computed as; [16]

$$P = df\,(DB) + OVB\,(Di - DB) \quad (4.12)$$

Di = depth of interest beneath the boundary, ft.

DB = depth of boundary, ft.

PP = pore pressure at Di, psi.

df =density of formation liquid, psi/ft.

OVB = overburden stress gradient, psi

4.2. The Methodology

In this project the calculation will be based on Eaton Method. The Eaton method has been described as a "horizontal" pressure method because it compares an in-situ physical property to a "normally-compacted" equivalent physical property at the same depth. This implies that the method is valid as long as the normal compaction trend can be constructed for all depths of interest. Before we use Equation (4.1), we need to prepare the following parameters:

4.2.1 Determination of Overburden Stress:

At a given depth, the overburden pressure is the pressure exerted by the cumulative weight of the overlying sediments. The cumulative weight of the overlying rocks is a function of the bulk density, the combined weight of matrix and formation fluids contained within the pore space.

Overburden Stress (OBG):

OBG (KPa) = ρb (g/cc) x TVD (m) x 9.8 …………………………………………… (4.13)

OBG (psi) = ρb (g/cc) x TVD (ft) x 0.433 ...………………………………………… (4.14)

4.2.2 Determination of Bulk Density:

Bulk density is a function of the matrix density, porosity and pore fluid density, and can be determined from the following formula:

$$\rho_b = \emptyset \rho_f + (1-\emptyset)\, \rho_m \quad \text{(4.15)}$$

Where:

$\emptyset$ = porosity.

ρ_f = pore fluid density.

ρ_m = matrix density.

Accurate determination of the overburden gradient is critical for accurate formation and fracture gradient calculations. Direct measurements of bulk density are preferable, so density values from wireline logs are extremely useful. However, this source of data is rarely available for an entire well interval. Finally, direct measurements from cuttings can be made while the well is being drilled.

4.2.3 Determination Hydrostatic Pressure:

Hydrostatic pressure is controlled by the density of the fluid saturating the formation. As the pore water becomes saline, or other dissolved solids are added, the hydrostatic pressure gradient will increase.

$$P_{hyd} = 0.052 * \rho * H \quad \text{(4.16)}$$

4.2.4 The Interval Velocity and Normal trend:

The rock velocity required for pore pressure estimation is a fundamental property that mainly depends on the grains, pores and the fluid properties and their interaction as well as the extrinsic property such as formation pressure and temperature. However, the interval velocities have been used to predict the pore pressure which obtained from the below pre-stack time migration, fig (4.1) of the following information:

i. Line: RSM07- 052,
ii. Area: Red sea, Sudan Date Shot: 2007.
iii. Sample interval: 4ms, samples/trace: 1750.
iv. Source type: air gun gun depth 5m
v. Record length: 8000ms.

Seismic velocities used during seismic processing are designed for accurate pore pressure prediction.

Interval velocities obtained from pre stack seismic data of common Depth point (CDP) gathers. A CDP gather is a collection of seismic traces for which the midpoint between the source and receiver for each Source / receiver pair in the gather lies at the same spatial location.

Interval velocities are derived from Dix's equation after picking the horizons in the semblance in the process of velocity analysis of pre stack time migrated (PSTM). The analysis showed an increase of interval velocity with depth, see figure (4.2). A normal trend of seismic interval velocities have been created and represented by a smooth curve. However lateral velocity variations resulting, for example, from dipping structures, lithology variations, salt layers of various thickness, fault blocks and variations in compaction and pore pressure cannot be accounted in the analysis.

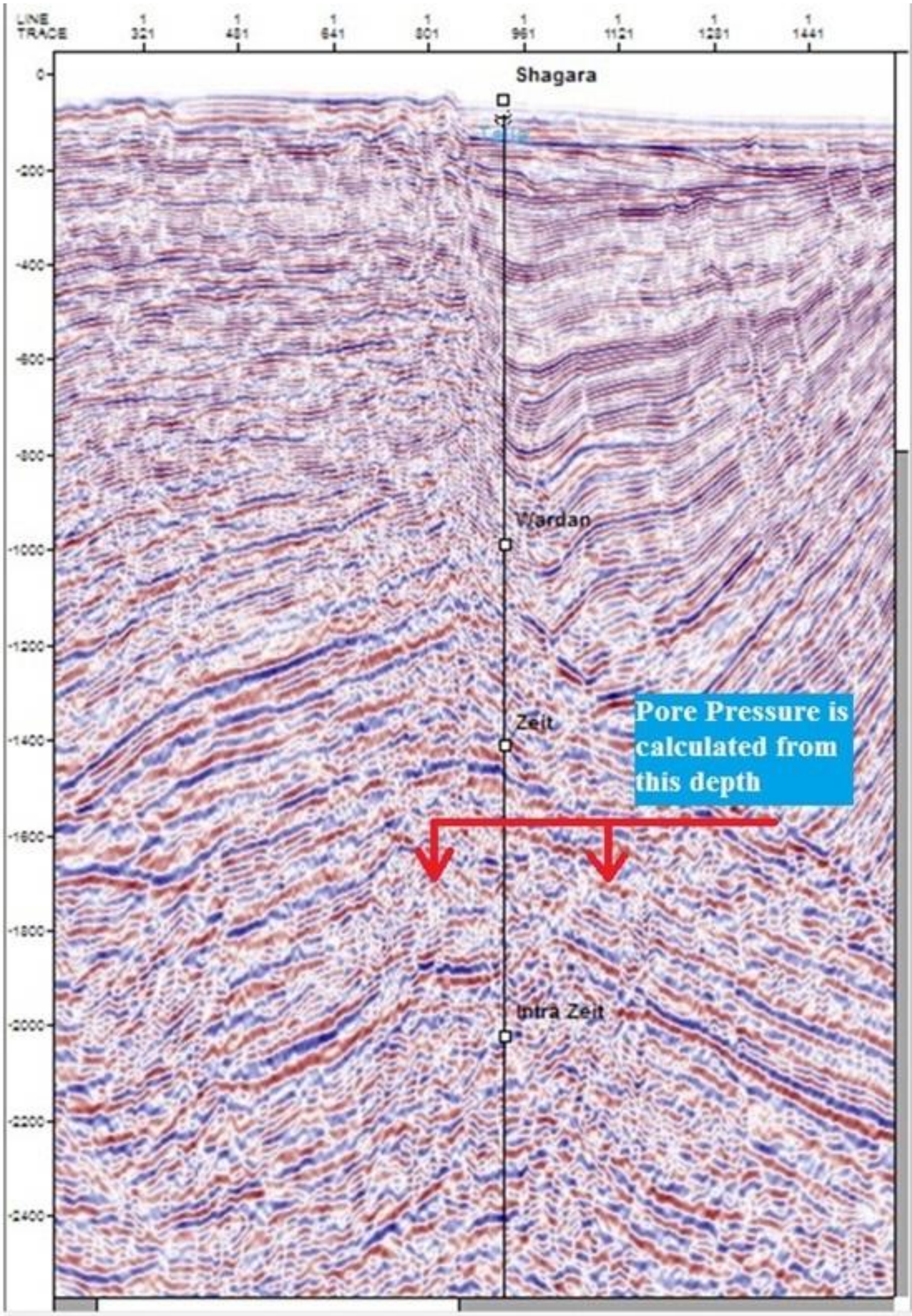

Fig (4.1): 2D seismic line showing the layers penetrated by Talla-1 well.

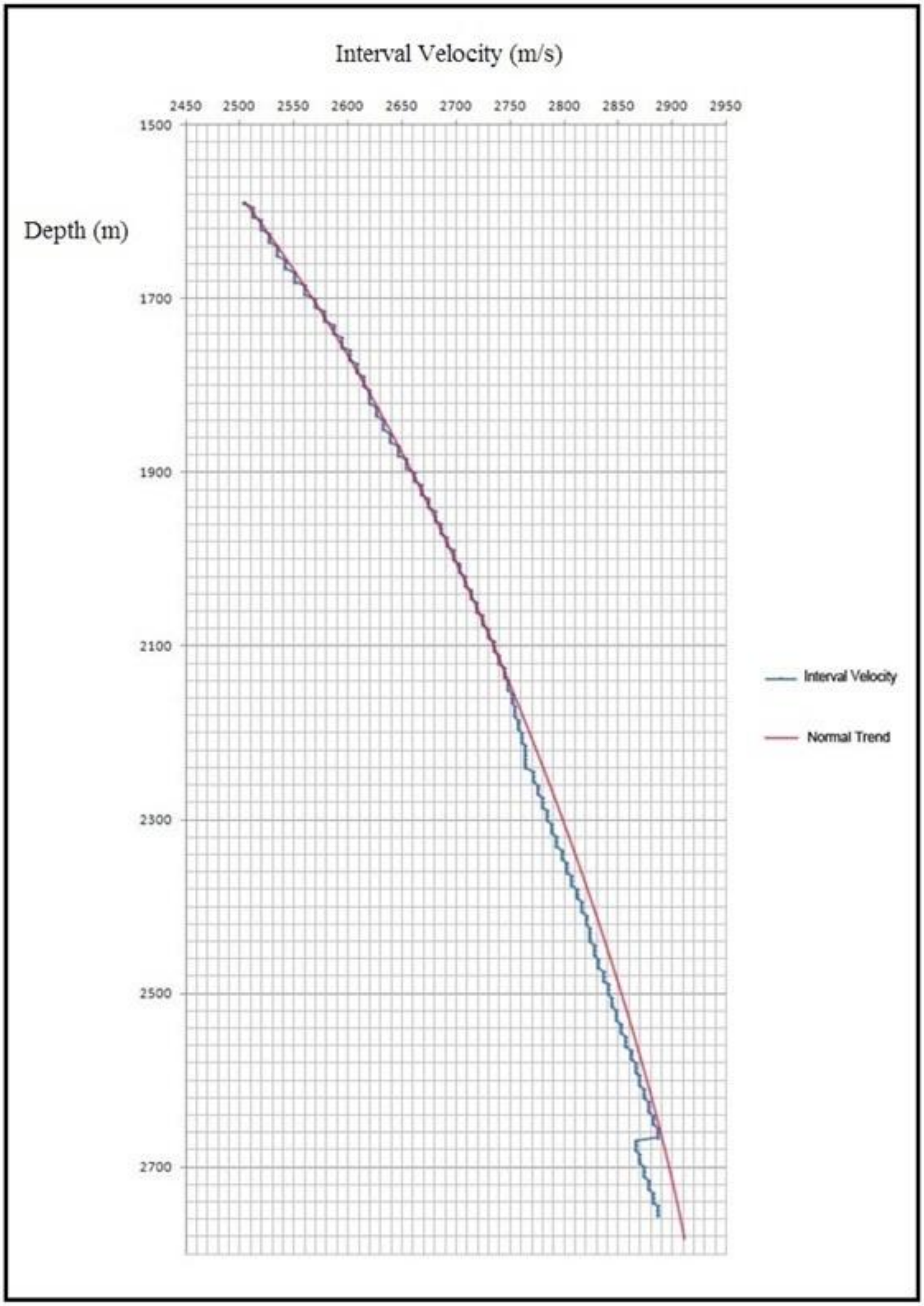

Fig(4.2): Interval Velocity increasing with depth is plotted and the normal trend of the velocity illustrated as the red curve.

Table (4.1): Values of parameters used to calculate pore pressure

Depth(ft)	RHOP(G/C3)	OBG(psi)	Phyd(psi)	Vint	Vnorm	PP Eaton
5216.79	2.061033811	4655.607588	2258.87007	2503.779	2514.35	2228.137923
5233.195	2.061868453	4672.13914	2265.973435	2511.555122	2514.35	2265.018954
5249.6	2.062703095	4688.68255	2273.0768	2511.555122	2514.35	2272.307608
5266.005	2.063537737	4705.237817	2280.180165	2511.555122	2514.35	2279.601498
5282.41	2.064372379	4721.804942	2287.28353	2519.037859	2527.294	2265.681661
5298.815	2.065207021	4738.383924	2294.386895	2519.037859	2527.294	2272.903809
5315.22	2.066041663	4754.974764	2301.49026	2519.037859	2527.294	2280.131469
5331.625	2.066876305	4771.577461	2308.593625	2526.425994	2527.294	2316.426977
5348.03	2.067710947	4788.192016	2315.69699	2526.425994	2534.366	2295.949061
5364.435	2.068545589	4804.818428	2322.800355	2526.425994	2534.366	2303.199239
5380.84	2.069380231	4821.456698	2329.90372	2533.915422	2534.366	2340.152424
5397.245	2.070214873	4838.106826	2337.007085	2533.915422	2534.366	2347.528663
5413.65	2.071049515	4854.768811	2344.11045	2533.915422	2539.579	2334.175894
5430.055	2.071884157	4871.442653	2351.213815	2541.505977	2539.579	2371.72853
5446.46	2.072718799	4888.128353	2358.31718	2541.505977	2539.579	2379.160566
5462.865	2.073553441	4904.825911	2365.420545	2541.505977	2539.579	2386.599608
5479.27	2.074388083	4921.535326	2372.52391	2549.776516	2547.672	2394.729061
5495.675	2.075222725	4938.256599	2379.627275	2549.776516	2547.672	2402.185186
5512.08	2.076057367	4954.989729	2386.73064	2549.776516	2547.672	2409.648818
5528.485	2.076892009	4971.734716	2393.834005	2559.300949	2547.672	2455.155222
5544.89	2.077726651	4988.491562	2400.93737	2559.300949	2554.715	2434.563601
5561.295	2.078561293	5005.260264	2408.040735	2559.300949	2554.715	2442.088036
5577.7	2.079395935	5022.040825	2415.1441	2568.922973	2554.715	2488.181257
5594.105	2.080230577	5038.833243	2422.247465	2568.922973	2554.715	2495.865747
5610.51	2.081065219	5055.637518	2429.35083	2568.922973	2560.344	2480.84518
5626.915	2.081899861	5072.453651	2436.454195	2577.867332	2560.344	2524.374078
5643.32	2.082734503	5089.281641	2443.55756	2577.867332	2560.344	2532.134047
5659.725	2.083569145	5106.121489	2450.660925	2577.867332	2560.344	2539.903522
5676.13	2.084403788	5122.973195	2457.76429	2586.142317	2570.922	2538.140985
5692.535	2.08523843	5139.836758	2464.867655	2586.142317	2570.922	2545.895174
5708.94	2.086073072	5156.712179	2471.97102	2586.142317	2570.922	2553.659483
5725.345	2.086907714	5173.599457	2479.074385	2594.135781	2570.922	2593.720762
5741.75	2.087742356	5190.498592	2486.17775	2594.135781	2578.255	2571.731484
5758.155	2.088576998	5207.409586	2493.281115	2594.135781	2578.255	2579.536656
5774.56	2.08941164	5224.332436	2500.38448	2601.091895	2578.255	2615.670732
5790.965	2.090246282	5241.267145	2507.487845	2601.091895	2578.255	2623.600518
5807.37	2.091080924	5258.21371	2514.59121	2601.091895	2587.368	2593.897436

5823.775	2.092395935	5276.383479	2521.694575	2607.96299	2587.368	2630.051735
5840.18	2.094431501	5296.394066	2528.79794	2607.96299	2587.368	2638.078373
5856.585	2.096467067	5316.433571	2535.901305	2607.96299	2587.368	2646.11802
5872.99	2.098502633	5336.501995	2543.00467	2614.375724	2593.657	2654.476004
5889.395	2.100538199	5356.599338	2550.108035	2614.375724	2593.657	2662.543938
5905.8	2.102573764	5376.7256	2557.2114	2614.375724	2593.657	2670.625749
5922.205	2.10460933	5396.88078	2564.314765	2619.958255	2593.657	2702.033045
5938.61	2.106644896	5417.064879	2571.41813	2619.958255	2599.043	2687.478184
5955.015	2.108680462	5437.277897	2578.521495	2619.958255	2599.043	2695.606438
5971.42	2.110716028	5457.519834	2585.62486	2619.958255	2599.043	2703.749825
5987.825	2.112751594	5477.790689	2592.728225	2625.843898	2599.043	2736.87509
6004.23	2.114787159	5498.090463	2599.83159	2625.843898	2607.256	2709.835718
6020.635	2.116822725	5518.419156	2606.934955	2625.843898	2607.256	2717.979757
6037.04	2.118858291	5538.776767	2614.03832	2632.037411	2607.256	2752.803742
6053.445	2.120893857	5559.163298	2621.141685	2632.037411	2607.256	2761.102042
6069.85	2.122929423	5579.578747	2628.24505	2632.037411	2617.265	2725.529132
6086.255	2.124964988	5600.023114	2635.348415	2638.532249	2617.265	2762.099768
6102.66	2.127000554	5620.496401	2642.45178	2638.532249	2617.265	2770.380827
6119.065	2.12903612	5640.998606	2649.555145	2638.532249	2617.265	2778.680297
6135.47	2.131071686	5661.52973	2656.65851	2645.698227	2623.326	2791.639235
6151.875	2.133107252	5682.089772	2663.761875	2645.698227	2623.326	2799.997541
6168.28	2.135142818	5702.678734	2670.86524	2645.698227	2623.326	2808.375552
6184.685	2.137178383	5723.296614	2677.968605	2653.323536	2623.326	2850.46646
6201.09	2.139213949	5743.943413	2685.07197	2653.323536	2630.825	2825.470379
6217.495	2.141249515	5764.61913	2692.175335	2653.323536	2630.825	2833.911396
6233.9	2.143285081	5785.323767	2699.2787	2660.892633	2630.825	2876.167373
6250.305	2.145320647	5806.057322	2706.382065	2660.892633	2630.825	2884.801152
6266.71	2.147356212	5826.819796	2713.48543	2660.892633	2634.785	2875.505107
6283.115	2.149391778	5847.611188	2720.588795	2667.830863	2634.785	2915.256058
6299.52	2.151427344	5868.431499	2727.69216	2667.830863	2634.785	2924.017287
6315.925	2.15346291	5889.280729	2734.795525	2667.830863	2634.785	2932.802973
6332.33	2.155498476	5910.158878	2741.89889	2673.959223	2642.134	2935.689909
6348.735	2.157534042	5931.065946	2749.002255	2673.959223	2642.134	2944.500317
6365.14	2.159569607	5952.001932	2756.10562	2673.959223	2642.134	2953.336773
6381.545	2.161605173	5972.966837	2763.208985	2679.857798	2642.134	2989.049197
6397.95	2.163640739	5993.96066	2770.31235	2679.857798	2651.124	2956.387857
6414.355	2.165676305	6014.983403	2777.415715	2679.857798	2651.124	2965.242473
6430.76	2.167711871	6036.035064	2784.51908	2685.853532	2651.124	3001.841004
6447.165	2.169747436	6057.115644	2791.622445	2685.853532	2651.124	3010.871982
6463.57	2.171783002	6078.225142	2798.72581	2685.853532	2656.132	2996.343041
6479.975	2.173818568	6099.36356	2805.829175	2691.419552	2656.132	3031.311457

6496.38	2.175854134	6120.530896	2812.93254	2691.419552	2656.132	3040.443645
6512.785	2.1778897	6141.72715	2820.035905	2691.419552	2656.132	3049.607694
6529.19	2.179925266	6162.952324	2827.13927	2697.105781	2663.256	3051.606782
6545.595	2.181960831	6184.206416	2834.242635	2697.105781	2663.256	3060.806158
6562	2.185149284	6208.765178	2841.346	2697.105781	2663.256	3070.20088
6578.405	2.18718485	6230.085297	2848.449365	2702.911138	2663.256	3107.001768
6594.81	2.189220416	6251.434335	2855.55273	2702.911138	2670.548	3081.220799
6611.215	2.191255982	6272.812291	2862.656095	2702.911138	2670.548	3090.529318
6627.62	2.193291547	6294.219167	2869.75946	2708.293788	2670.548	3125.741038
6644.025	2.195327113	6315.654961	2876.862825	2708.293788	2670.548	3135.232724
6660.43	2.197362679	6337.119673	2883.96619	2708.293788	2676.856	3113.808829
6676.835	2.199398245	6358.613305	2891.069555	2713.797547	2676.856	3150.014784
6693.24	2.201433811	6380.135855	2898.17292	2713.797547	2676.856	3159.607951
6709.645	2.203469376	6401.687324	2905.276285	2713.797547	2676.856	3169.242689
6726.05	2.205504942	6423.267712	2912.37965	2718.884494	2680.758	3184.447135
6742.455	2.207540508	6444.877018	2919.483015	2718.884494	2680.758	3194.190665
6758.86	2.209576074	6466.515243	2926.58638	2718.884494	2680.758	3203.97867
6775.265	2.21161164	6488.182387	2933.689745	2724.104393	2680.758	3239.486227
6791.67	2.213647206	6509.87845	2940.79311	2724.104393	2687.895	3213.683025
6808.075	2.215682771	6531.603431	2947.896475	2724.104393	2687.895	3223.569529
6824.48	2.217718337	6553.357332	2954.99984	2729.258805	2687.895	3259.19801
6840.885	2.219753903	6575.14015	2962.103205	2729.258805	2687.895	3269.287476
6857.29	2.221432794	6595.892848	2969.20657	2729.258805	2693.156	3252.575226
6873.695	2.221684988	6612.423104	2976.309935	2734.357856	2693.156	3288.027276
6890.1	2.221937182	6628.956942	2983.4133	2734.357856	2693.156	3297.953701
6906.505	2.222189376	6645.494363	2990.516665	2734.357856	2693.156	3307.933086
6922.91	2.22244157	6662.035367	2997.62003	2739.40333	2700.456	3306.036432
6939.315	2.222693764	6678.579954	3004.723395	2739.40333	2700.456	3316.094708
6955.72	2.222945958	6695.128124	3011.82676	2739.40333	2700.456	3326.2097
6972.125	2.223198152	6711.679876	3018.930125	2744.039666	2700.456	3359.890851
6988.53	2.223450346	6728.235212	3026.03349	2744.039666	2706.124	3340.937401
7004.935	2.22370254	6744.79413	3033.136855	2744.039666	2706.124	3351.216051
7021.34	2.223954734	6761.356631	3040.24022	2748.103785	2706.124	3382.331436
7037.745	2.224206928	6777.922715	3047.343585	2748.103785	2706.124	3392.788668
7054.15	2.224459122	6794.492382	3054.44695	2748.103785	2712.567	3369.699618
7070.555	2.224711316	6811.065632	3061.550315	2751.598528	2712.567	3398.251361
7086.96	2.22496351	6827.642464	3068.65368	2751.598528	2712.567	3408.868896
7103.365	2.225215704	6844.222879	3075.757045	2751.598528	2712.567	3419.556142
7119.77	2.225467898	6860.806878	3082.86041	2754.358716	2724.522	3381.529921
7136.175	2.225720092	6877.394459	3089.963775	2754.358716	2724.522	3392.239009
7152.58	2.225972286	6893.985623	3097.06714	2754.358716	2724.522	3403.022727

7168.985	2.22622448	6910.580369	3104.170505	2757.089244	2724.522	3428.297502
7185.39	2.226476674	6927.178699	3111.27387	2757.089244	2730.657	3406.386031
7201.795	2.226728868	6943.780612	3118.377235	2757.089244	2730.657	3417.358311
7218.2	2.226981062	6960.386107	3125.4806	2759.956977	2730.657	3443.724645
7234.605	2.227233256	6976.995185	3132.583965	2759.956977	2730.657	3454.900358
7251.01	2.22748545	6993.607846	3139.68733	2759.956977	2736.445	3434.751999
7267.415	2.227737644	7010.22409	3146.790695	2763.133858	2736.445	3463.163867
7283.82	2.227989838	7026.843917	3153.89406	2763.133858	2736.445	3474.567196
7300.225	2.228242032	7043.467326	3160.997425	2763.133858	2736.445	3486.062265
7316.63	2.228494226	7060.094319	3168.10079	2763.133858	2740.389	3476.021018
7333.035	2.22874642	7076.724894	3175.204155	2763.133858	2740.389	3487.653063
7349.44	2.228998614	7093.359052	3182.30752	2763.133858	2740.389	3499.383371
7365.845	2.229250808	7109.996793	3189.410885	2771.089994	2740.389	3554.588567
7382.25	2.229503002	7126.638117	3196.51425	2771.089994	2745.689	3537.464577
7398.655	2.229755196	7143.283024	3203.617615	2771.089994	2745.689	3549.538349
7415.06	2.23000739	7159.931514	3210.72098	2775.170267	2745.689	3584.056338
7431.465	2.230259584	7176.583586	3217.824345	2775.170267	2745.689	3596.402088
7447.87	2.230511778	7193.239241	3224.92771	2775.170267	2750.278	3583.376637
7464.275	2.230763972	7209.898479	3232.031075	2779.545692	2750.278	3619.992716
7480.68	2.231016166	7226.5613	3239.13444	2779.545692	2750.278	3632.681383
7497.085	2.23126836	7243.227704	3246.237805	2779.545692	2750.278	3645.490915
7513.49	2.231520554	7259.897691	3253.34117	2783.877477	2754.096	3661.034388
7529.895	2.231772748	7276.57126	3260.444535	2783.877477	2754.096	3674.100376
7546.3	2.232024942	7293.248413	3267.5479	2783.877477	2754.096	3687.295856
7562.705	2.232277136	7309.929148	3274.651265	2788.330408	2754.096	3725.256449
7579.11	2.23252933	7326.613466	3281.75463	2788.330408	2760.986	3700.108662
7595.515	2.232781524	7343.301367	3288.857995	2788.330408	2760.986	3713.677825
7611.92	2.233033718	7359.992851	3295.96136	2792.910081	2760.986	3752.951593
7628.325	2.233285912	7376.687918	3303.064725	2792.910081	2760.986	3766.868267
7644.73	2.233538106	7393.386567	3310.16809	2792.910081	2767.521	3743.881329
7661.135	2.2337903	7410.088799	3317.271455	2797.778254	2767.521	3785.404484
7677.54	2.234042494	7426.794615	3324.37482	2797.778254	2767.521	3799.754647
7693.945	2.234294688	7443.504013	3331.478185	2797.778254	2767.521	3814.264046
7710.35	2.234546882	7460.216994	3338.58155	2801.937074	2771.525	3829.561916
7726.755	2.234799076	7476.933557	3345.684915	2801.937074	2771.525	3844.402432
7743.16	2.23505127	7493.653704	3352.78828	2801.937074	2771.525	3859.413546
7759.565	2.235303464	7510.377433	3359.891645	2806.710663	2771.525	3901.560464
7775.97	2.235555658	7527.104746	3366.99501	2806.710663	2776.889	3886.277268
7792.375	2.235807852	7543.835641	3374.098375	2806.710663	2776.889	3901.815808
7808.78	2.236060046	7560.570119	3381.20174	2812.106629	2776.889	3948.189312
7825.185	2.23631224	7577.30818	3388.305105	2812.106629	2776.889	3964.176888

7841.59	2.236564434	7594.049824	3395.40847	2812.106629	2782.442	3948.331012
7857.995	2.236816628	7610.79505	3402.511835	2816.302577	2782.442	3988.625311
7874.4	2.237068822	7627.54386	3409.6152	2816.302577	2782.442	4005.195561
7890.805	2.237321016	7644.296252	3416.718565	2816.302577	2782.442	4021.975621
7907.21	2.23757321	7661.052227	3423.82193	2819.96674	2788.864	4022.705711
7923.615	2.237825404	7677.811785	3430.925295	2819.96674	2788.864	4039.883069
7940.02	2.238077598	7694.574926	3438.02866	2819.96674	2788.864	4057.285197
7956.425	2.238329792	7711.341649	3445.132025	2823.748987	2788.864	4096.738926
7972.83	2.238581986	7728.111956	3452.23539	2823.748987	2792.562	4093.033959
7989.235	2.23883418	7744.885845	3459.338755	2823.748987	2792.562	4111.142802
8005.64	2.239086374	7761.663318	3466.44212	2823.748987	2792.562	4129.498057
8022.045	2.239338568	7778.444373	3473.545485	2827.178259	2792.562	4168.048356
8038.45	2.239590762	7795.229011	3480.64885	2827.178259	2797.145	4159.93066
8054.855	2.239842956	7812.017231	3487.752215	2827.178259	2797.145	4179.04426
8071.26	2.24009515	7828.809035	3494.85558	2831.222006	2797.145	4222.101953
8087.665	2.240347344	7845.604422	3501.958945	2831.222006	2797.145	4241.815046
8104.07	2.240599538	7862.403391	3509.06231	2831.222006	2801.873	4233.697795
8120.475	2.240851732	7879.205943	3516.165675	2835.714074	2801.873	4280.375024
8136.88	2.241103926	7896.012078	3523.26904	2835.714074	2801.873	4300.952759
8153.285	2.24135612	7912.821796	3530.372405	2835.714074	2801.873	4321.833546
8169.69	2.241608314	7929.635097	3537.47577	2840.162426	2806.783	4339.952191
8186.095	2.241860508	7946.451981	3544.579135	2840.162426	2806.783	4361.453594
8202.5	2.242112702	7963.272447	3551.6825	2840.162426	2806.783	4383.279682
8218.905	2.242364896	7980.096496	3558.785865	2844.09169	2806.783	4428.694334
8235.31	2.24261709	7996.924128	3565.88923	2844.09169	2810.672	4427.900709
8251.715	2.242869284	8013.755344	3572.992595	2844.09169	2810.672	4450.746779
8268.12	2.244202309	8034.459622	3580.09596	2847.98447	2810.672	4497.309112
8284.525	2.247456813	8062.075562	3587.199325	2847.98447	2810.672	4521.479831
8300.93	2.250711316	8089.737739	3594.30269	2847.98447	2814.043	4525.530282
8317.335	2.25396582	8117.446151	3601.406055	2852.640596	2814.043	4578.400802
8333.74	2.257220323	8145.2008	3608.50942	2852.640596	2814.043	4603.756508
8350.145	2.260474827	8173.001684	3615.612785	2852.640596	2814.043	4629.513811
8366.55	2.26372933	8200.848804	3622.71615	2856.786882	2821.057	4637.662308
8382.955	2.266983834	8228.74216	3629.819515	2856.786882	2821.057	4664.169049
8399.36	2.270238337	8256.681752	3636.92288	2856.786882	2821.057	4691.105715
8415.765	2.273492841	8284.667579	3644.026245	2861.205864	2821.057	4745.680506
8432.17	2.276747344	8312.699643	3651.12961	2861.205864	2826.246	4741.127537
8448.575	2.280001848	8340.777942	3658.232975	2861.205864	2826.246	4769.391292
8464.98	2.283256351	8368.902477	3665.33634	2865.586398	2826.246	4825.444087
8481.385	2.286510855	8397.073248	3672.439705	2865.586398	2826.246	4854.78327
8497.79	2.289765358	8425.290255	3679.54307	2865.586398	2830.467	4857.729721

8514.195	2.293019861	8453.553498	3686.646435	2869.613763	2826.246	4940.221008
8530.6	2.464403695	9102.890656	3693.7498	2869.613763	2826.246	5007.886634
8547.005	2.467658199	9132.440654	3700.853165	2869.613763	2826.246	5039.452312
8563.41	2.470912702	9162.036889	3707.95653	2873.917448	2833.125	5052.383893
8579.815	2.474167206	9191.679359	3715.059895	2873.917448	2833.125	5084.964785
8596.22	2.477421709	9221.368065	3722.16326	2873.917448	2833.125	5118.111816
8612.625	2.480676212	9251.103007	3729.266625	2877.873711	2833.125	5180.455292
8629.03	2.483930716	9280.884184	3736.36999	2877.873711	2839.245	5169.748586
8645.435	2.48393	9298.525771	3743.473355	2877.873711	2839.245	5203.965466
8661.84	2.490439723	9340.585247	3750.57672	2881.951744	2839.245	5269.996634
8678.245	2.493694226	9370.505132	3757.680085	2881.951744	2839.245	5306.231795
8694.65	2.49694873	9400.471253	3764.78345	2881.951744	2843.032	5314.735256
8711.055	2.500203233	9430.48361	3771.886815	2885.995347	2843.032	5382.140899
8727.46	2.503457737	9460.542203	3778.99018	2885.995347	2843.032	5420.376449
8743.865	2.50671224	9490.647032	3786.093545	2885.995347	2843.032	5459.307856
8760.27	2.509966744	9520.798096	3793.19691	2865.586398	2848.38	5301.759817
8776.675	2.513221247	9550.995397	3800.300275	2865.586398	2848.38	5341.336607
8793.08	2.516475751	9581.238933	3807.40364	2865.586398	2848.38	5381.657175
8809.485	2.519730254	9611.528705	3814.507005	2869.613763	2848.38	5454.440733
8825.89	2.522984758	9641.864713	3821.61037	2869.613763	2852.379	5464.632482
8842.295	2.526239261	9672.246956	3828.713735	2869.613763	2852.379	5507.289798
8858.7	2.529001386	9700.786761	3835.8171	2873.917448	2852.379	5584.935235
8875.105	2.53026836	9723.620064	3842.920465	2873.917448	2852.379	5629.152014
8891.51	2.530538568	9742.63379	3850.02383	2873.917448	2856.054	5644.583209
8907.915	2.530808776	9761.651355	3857.127195	2877.873711	2856.054	5721.955351
8924.32	2.531078984	9780.672759	3864.23056	2877.873711	2856.054	5768.680862
8940.725	2.531349192	9799.698002	3871.333925	2877.873711	2856.054	5816.319947
8957.13	2.5316194	9818.727083	3878.43729	2881.951744	2860.08	5865.064007
8973.535	2.531889607	9837.760003	3885.540655	2881.951744	2860.08	5914.594831
8989.94	2.532141801	9856.726641	3892.64402	2881.951744	2860.08	5965.102374
9006.345	2.532393995	9875.696861	3899.747385	2885.995347	2860.08	6049.029994
9022.75	2.532646189	9894.670664	3906.85075	2885.995347	2866.982	6045.67487
9039.155	2.532898383	9913.64805	3913.954115	2885.995347	2866.982	6099.211056

4.3 The Results:

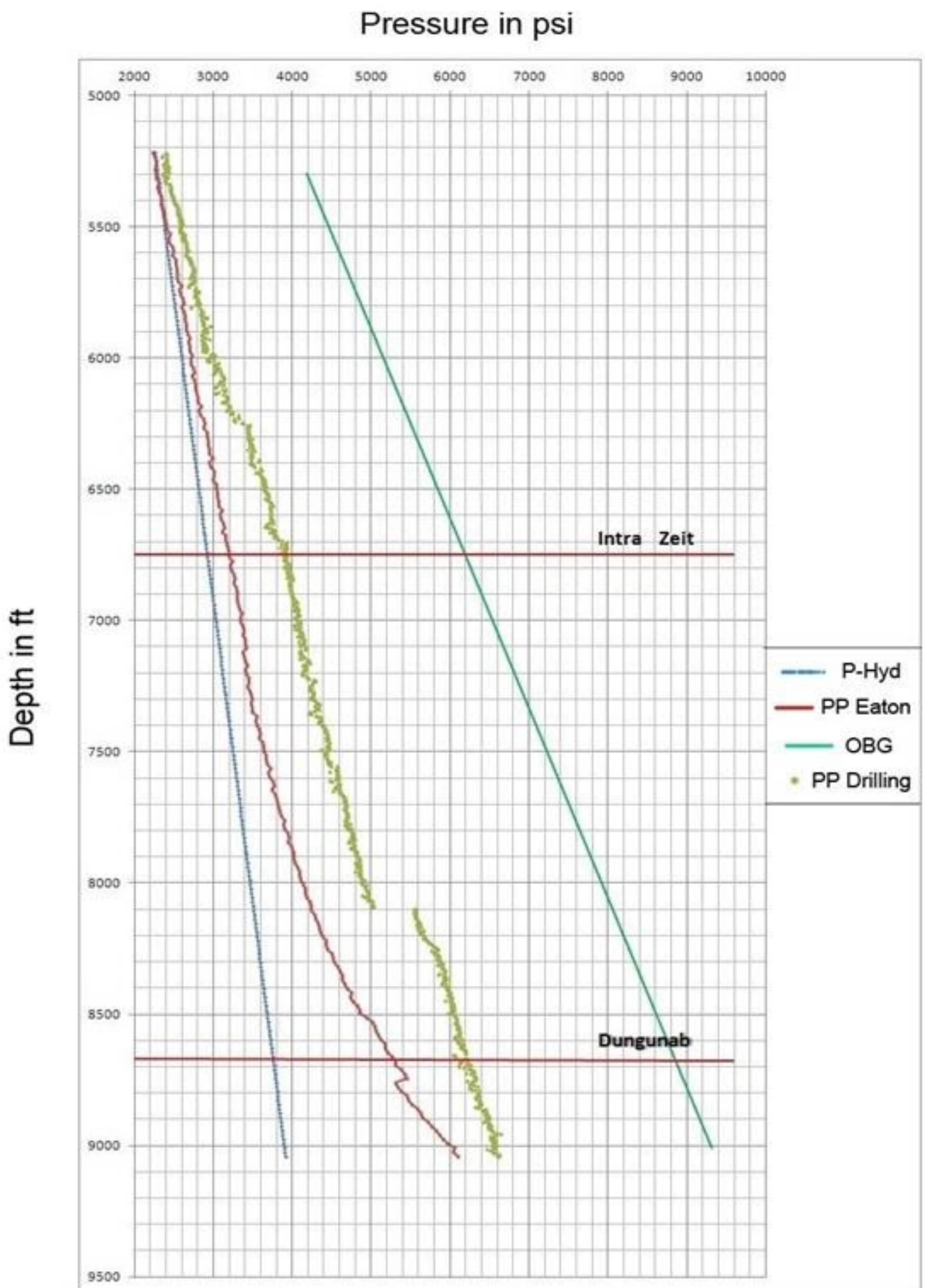

Fig (4.3) : Pore Pressure Predicted using Eaton method plotted with depth

4.4 Discussion:

As shown in the results in Fig (4.3), a cross plot has been made between pressure predicted applying Eaton method using equation (4.1) with depth also a pressure values from drilling information was added to the plot to be compared with predicted values.

The required inputs have been added to excel and the output is in the last column of table (4.1) which is PP Eaton.

The prediction of pore pressure has been made at depths from 1590m to 2775m according to the available data of well logs at those depths.

Since the pressure at those depths increase smoothly there is no evidence of abnormal pressures could be encountered.

Chapter Five

Conclusion & Recommendation

Chapter Five

Conclusions & Recommendations

5.1 Conclusions:

1. Four of expected formations were penetrated in Talla-1. They were Shagara, Wardan, Zeit and Dungunab formations.
2. There are errors that can slip into the seismic data from different sources: geology, acquisition parameters and processing. From a geological perspective the problems can arise from salt, dipping beds, velocity lateral variation or thick homogeneous intervals that display no reflectivity.
3. The geological studies show that a salt layer was encountered at depth 2638.8m TVDss, which considered the trouble formation.
4. Because of the uncertainties in velocity estimation which increase with the geological complexity and depth. Therefore, the accuracy of values of pore pressure predicted is moderate but reasonable as it has been shown in the figure.
5. One can conclude that there is no evidence of abnormal pressure at the depths have been studied.

5.2 Recommendations:

1. We recommended using dense and accurate seismic velocities that are close to the formation velocities under consideration to predict pore pressure.
2. We recommended developing software for pressure prediction which is relatively limited to simplify the calculations.
3. We recommended doing more studies of pore pressures in the area studied.

References:

1. Bikas Kumar, Sri Niwas, Bikram K. Mangaraj, (2012). Pore Pressure Prediction from Well Logs and Seismic Data. Biennial International Conference & Exposition on Petroleum Geophysics. SPG Paper 005.
2. Chatterjee, Avirup, Mondal, Samit, Basu, Pramit, Patel, B.K., (2012). Pore Pressure Prediction Using Seismic Velocities for deep water High Temperature - High Pressure well in offshore Krishna Godavari Basin, India. SPE Oil and Gas India Conference and Exhibition. Paper SPE 153764.
3. Ekwo Ernest Uchechukwu M.Sc. Thesis. (2014). Pore Pressure Prediction: A Case Study of Sandstone Reservoir, Bredaasdorp Basin, South Africa.
4. G. Z. Ugwu, (2015). An overview of pore pressure prediction using seismically derived velocities. Journal of Geology and Mining Research. Vol. 7(4), pp. 31-40.
5. https://www.scribd.com/doc/57664091/17/Calculation-of-Overburden-Gradient
6. http://www.scribd.com/doc/57664091/Formation-Pressure-v2-1
7. http://csegrecorder.com/articles/view/velocity-determination-for-pore-pressure-prediction
8. Jwngsar Brahma, Anirbid Sircar, G. P. Karmakar, (2013). Pre-drill pore pressure prediction using seismic velocities data on flank and synclinal part of Atharamura anticline in the Eastern Tripura, India. Journal of Petroleum Exploration and Production Technologies Vol. 3(2).
9. Mohammed Salah M.Sc. Research, (2012). Interpretation of Gravity and Remote Sensing Data for Improved Geological Mapping North of Port Sudan Area.
10. Orapan Limpornpipat, Andrew Laird, Mark Tingay, Christopher K. Morley, Chaiwat Kaewla, Hamish Macintyre, (2011). Overpressures in the Northern Malay Basin: Part2 - Implication for Pore Pressure Prediction. IPTC SPE Paper 15350.
11. P. Avseth, T. Mukerji and G. Mavko, (2005) Quantitative Seismic Interpretation. United Kingdom: Cambridge University Press.
12. PETROServices ," TALLA-1 End of Well Report_Final", Sudan. October 2010.
13. PETROServices . "Talla-1 Final Pressure Data". Khartoum, Sudan. October 2010.
14. BPC processing center, Pre-stack time migration, Khartoum, Sudan. 2006.

15. http://ocw.utm.my/file.php/61/To_upload_OCW_Formation_pressures.pdf.
16. Jagadeesh Kilaparthi, 2013. The Implementation of a Pore Pressure and Fracture Gradient Prediction Model for the North Sea Centeral Judy and Jade Fields. Department of Geography, Environment and Society, Coventry University
17. Sayers, C.M., Johnson, G.M., Denyer, G., (2000). Predrill Pore Pressure Prediction Using Seismic Data. SPE Drilling Conference - New Orleans, Louisiana. Paper SPE 59122.
18. Wawan A. Behaki, Aldyth Sukapradja, Ronald C. Siregar, Radig Wisnu Y., Setiabundi Djaelani, Benny A. Sjafwan, (2012). 3D Pore Pressure Prediction Model in Bentu Block – Central Sumatra Basin. AAPG International Convention and Exhibition, Singapore. Article 41105.
19. Yully P. Solano, Rodolfo Uribe, Marcelo Frydman, Nestor F. Saavedra, Zuly H. Calderon, (2007). A modified Approach to Predict Pore Pressure Using the DExponent Method: An Example from The Carbonera Formation, Colombia.